Biogeochemistry
https://doi.org/10.1007/s10533-020-00675-6

Trade-off between 'new' SOC stabilisation from above-ground inputs and priming of native C as determined by soil type and residue placement

Elaine Mitchell · Clemens Scheer · David Rowlings · M. Francesca Cotrufo · Richard T. Conant · Johannes Friedl · Peter Grace

Received: 15 October 2019 / Accepted: 9 May 2020

Abstract Due to the geographical expanse of grasslands with depleted organic matter stocks, there has been growing interest in the management of these ecosystems for C sequestration to help mitigate climate change. It is generally accepted that management practices intending to increase forage production (e.g. decreasing grazing density) result in increased soil C stocks by increasing the return of biomass inputs to the soil organic carbon (SOC) pool. However, the contribution of C inputs to stable SOC versus GHG losses, and how this is affected by soil properties, remains largely unknown, particularly within subtropical biomes. To investigate the role of soil texture and mineralogy on SOC stabilisation, we identified three different soil types with varying physical properties in close proximity (< 2 km^2) to each other. We used isotopically labelled plant material (^{13}C), placed on the soil surface versus incorporated within the mineral soil, to trace the fate of fresh residue inputs into SOM fractions that differed in their degree of protection and mechanistic interactions with the soil matrix. Weekly GHG measurements (CO_2, N_2O and CH_4) were taken to understand the overall GHG balance resulting from C inputs (i.e. SOC accrual versus GHG losses in CO_2 equivalents). In finer textured soils with a greater smectite content, SOC accrual was greater but was significantly outweighed by GHG losses, primarily from native SOC priming. The incorporation of residue within the soil increased residue-derived SOC accrual by 4- to 5-fold, whilst also suppressing the priming of native SOC. This improved understanding of how soil texture and residue placement affect the global warming mitigation potential of subtropical grassland soils will be important in determining identifiable regions that should be targeted for SOC restoration efforts by increasing C inputs.

Keywords Decomposition · Stable isotopes · Soil texture · C priming effect · SOC stabilisation · C sequestration · GHG fluxes · Climate change mitigation

Responsible Editor: Sharon A. Billings

Electronic supplementary material The online version of this article (https://doi.org/10.1007/s10533-020-00675-6) contains supplementary material, which is available to authorized users.

E. Mitchell (✉)
Institute for Future Environments, Queensland University of Technology, Level 7, P Block, Gardens Point Campus, 2 George Street, Brisbane, QLD 4000, Australia
e-mail: e5.mitchell@qut.edu.au

C. Scheer · D. Rowlings · J. Friedl · P. Grace
Institute for Future Environments, Queensland University of Technology, Brisbane, QLD, Australia

M. F. Cotrufo · R. T. Conant
Natural Resource Ecology Laboratory, Colorado State University, Fort Collins, CO, USA

Published online: 19 May 2020

Introduction

Grasslands cover more than 30% of terrestrial lands (Derner and Schuman 2007), with livestock grazing as the primary, and often only viable economic use, supporting the livelihoods of approximately 1 billion people (Sayre et al. 2013). Due to the geographical expanse of grasslands with depleted soil organic carbon (SOC) stocks (~ 11% of Australia's 49 M ha of grassland is considered degraded, (Conant and Paustian 2002)) there has been growing interest in the management of these ecosystems for C sequestration to help mitigate climate change (Asner et al. 2004; Conant et al. 2017; Lipper et al. 2010; Morgan et al. 2010; Ryals et al. 2014), whilst improving ecosystem services (Byrnes et al. 2018).

It is generally accepted that management practices intending to increase forage production (e.g. decreasing grazing density) result in increased SOC stocks by increasing the return of biomass inputs to the SOC pool (Conant et al. 2017). The majority of these C inputs are mineralised by soil microorganisms and respired to the atmosphere over short time scales. However, a portion of added C cycles slowly through the soil, persisting for decades, centuries or even millennia as it is 'protected' from further microbial degradation (Krull et al. 2003; Trumbore 2000). Understanding how biomass inputs contribute to 'protected' versus 'unprotected' SOC allow inferences to be made on the likely persistence and functioning of the SOC accrued from increased C inputs (Lavallee et al. 2019).

A key mechanism for the protection or stabilisation of C in soils is by chemical interactions with soil minerals, particularly silt and clay particles (Kleber et al. 2015; Six et al. 2002; Torn et al. 1997). The presence of sorptive mineral surfaces also contribute to the formation of soil aggregates that encapsulate SOC, physically separating C from the decomposer community, whilst limiting the diffusion of oxygen, water and enzymes required for the breakdown of organic matter (Six et al. 2002). The reactivity of clay minerals is also dependent on their type (expandable 2:1 versus non expandable 2:1 or 1:1 phyllosilicate clay minerals) with, for example, soils rich in smectite protecting more OC than kaolinite rich soils (Hassink 1997; Wattel-Koekkoek et al. 2001).

Labile plant inputs are thought to be important in the accumulation of stable SOC as they are readily accessed and efficiently used by soil microbes, with the eventual microbial necromass forming an important precursor to stable SOC (Cotrufo et al. 2013). Paradoxically, these same labile inputs may stimulate microbial decomposition of native SOC (the C priming effect) (Fontaine et al. 2004; Jenkinson et al. 1985; Kuzyakov 2000), resulting in the mineralisation of native C to gaseous or soluble forms that are then lost from the soil system. Priming may enhance the decomposition of 'unprotected' native SOC or may act to destabilise 'protected' SOC. For example, low molecular weight organic acids released as dissolved organic carbon (DOC) can destabilise native adsorbed SOC from mineral surfaces (Kaiser and Kalbitz 2012). Enhanced decomposition of native SOC can persist long after the exhaustion of the added organic matter, ultimately resulting in a net carbon loss (Fontaine et al. 2004; Ohm et al. 2007). Furthermore, labile plant inputs may also affect soil microbial populations responsible for processes such as denitrification (Azam et al. 2002; Morley and Baggs 2010; Weier et al. 1993) and methane consumption (Goldman et al. 1995).

In this study we aim to further the understanding of C inputs and their effect on the balance between the processes SOC stabilisation and destabilisation (C priming) as a function of soil type and residue placement. This was presented as an overall GHG balance (expressed in CO_2 equivalents) through the inclusion of N_2O and CH_4 fluxes that occurred as a result of residue addition. Residue placement was manipulated (surface applied versus incorporated within soil) to provide a greater process level understanding of how the placement of residue interacts with soil properties to alter the GHG balance. Embedding residue within the soil potentially mimics the impact of animal trampling which has been reported to enhance the physical break down and incorporation of plant residue in the mineral soil (Sanjari et al. 2008; Schuman et al. 1999; Southorn 2002), with grazing management strategies (e.g. adaptive multi-paddock grazing (Provenza, 2008)) affecting the distribution and intensity of trampling.

We hypothesise that soil physical properties will be a strong determinant of residue decomposition through their control on the soil moisture content in semi-arid grassland soils. Finer textured soils will favour greater soil moisture retention and hydraulic connectivity, meaning that microsites of potential decomposition

are more readily connected with one another for the diffusion of C and other resources such as enzymes and nutrients required for decomposition (Guo et al. 2012). Greater residue decomposition in finer textured soils will result in a greater transfer of labile residue to the soil, which will likely increase SOC stabilisation as mineral-associated organic matter (MAOM) (Cotrufo et al. 2013). Labile C may also increase native SOC priming, but this may be supressed in finer textured soils as due to the greater protection of SOC by mineral surfaces—thereby limiting the access of SOC and nutrients to soil microorganisms and their enzymes (Dungait et al. 2012; Six et al. 2002). A greater availability of labile C and N, combined with higher soil moisture content in finer textured soils, may also affect microbially mediated processes such as denitrification and methane consumption. We expected that the incorporation of residue will amplify the above effects, as the incorporation of residue will expedite the transfer of above-ground inputs to all SOC fractions (Mitchell et al. 2016, 2018). It is expected that the mixing of residue within the soil will increase the priming of native SOC by disrupting soil structure thereby exposing new surfaces to microbial attack (Six et al. 1999). A greater understanding of how soil texture and residue placement affect the overall GHG balance of semi-arid grassland soils is an important step in identifying regions that should be targeted for SOC restoration efforts.

Methods

Experimental site

This experiment leveraged the work of a previous experiment that was conducted on a vertisol on a long-term pasture near Crows Nest, Queensland, Australia (27° 16′ S 152° 03′ E) (Mitchell et al. 2018). This experiment used two additional pasture soils within close proximity to the original site (all sites < 2 km apart) that varied in soil texture and mineralogical properties. The three different soil types, hereafter referred to as CLAY, LOAM and SAND, were classified according to the USDA soil texture survey (Soil Survey Division Staff 1993) (Table 1). Livestock were excluded from the study sites by temporary fences for the duration of the experiment (February 2014–February 2015). The climate is subtropical with warm wet summers and dry winters with a mean annual temperature of 17 °C. Total precipitation over the experimental period was 665 mm, with the highest levels of rainfall received in the summer months (December–February). Soil bulk density (BD) on the three different soil types was determined on four replicates by the soil core (10 cm) method. Temperature was measured using HOBO data loggers (Onset, Bourne, Maryland, USA) placed at a depth of 10 cm for each soil type and daily rainfall was collected using a manual rain gauge.

Isotopically labelled residue production and analyses

To trace fresh residue-derived C into SOM fractions that varied in their turnover time, ^{13}C labelled Rhodes grass tops (*Chloris gayana*) were used as this was the dominant grass species at the site. The grass was grown within a continuous labelling chamber under controlled conditions, as described in Mitchell et al. (2016). Once the Rhodes grass had reached maturity, the chamber was opened and aboveground biomass was cut at 10 cm from the soil surface. This biomass residue was then air-dried, cut to 10 cm pieces and homogenised. Residue moisture content was measured on three oven-dried (60 °C) subsamples for dry weight correction. The oven-dried subsamples were mill-ground and used for the determination of C (44%) and N (3.1%) concentrations and their isotopic composition (^{13}C = 3.8 atom %) by elemental analysis and isotope ratio mass spectrometry (EA-IRMS, Sercon Limited, UK).

Experimental design

On 13 February 2014, the air-dried labelled residue (10 cm strips) was placed inside PVC collars (10 cm in diameter, 15 cm height) inserted to a depth of 10 cm at a rate of 10 t ha^{-1} in the same experimental set up as described in Mitchell et al. (2018). Aboveground vegetation had been previously removed from inside the collars by clipping. Collars were covered by a 2 mm polyethylene mesh to prevent loss of the labelled residue or input of external plant material.

To explore the effect of soil properties and residue placement on residue-derived SOM formation and associated GHG fluxes, we established a two-way fully factorial experiment. Factor 1 explored the effect

Table 1 Selected properties for the 3 soil types at Crows Nest site (CLAY, LOAM, SAND) at depth 0–10 cm

Soil name	CLAY	LOAM	SAND
Soil texture (% composition)			
Sand (coarse) (250–1000 μm)	0	9.1	16.3
Sand (medium) (100–250 μm)	5.4	23.1	26.2
Sand (fine) (50–100 μm)	12.8	16.1	18.1
Silt (coarse) (20–50 μm)	11.2	8.4	5.2
Silt (fine) (2-20 μm)	21.7	11.2	5.1
Clay (< 2 μm)	49.2	31.2	30.1
pH (water)	5.3	5.1	5.1
Organic C (%)	3.7 (± 0.2)	3.3 (± 0.3)	1.9 (± 0.3)
C: N	12.9	10.4	13.1
POM (% of TOC)	15 (± 3.3)	27 (± 3.5)	36 (2.5)
SA (% of TOC)	4 (± 1.8)	8 (± 1.9)	3 (1.2)
SC (% of TOC)	81 (± 4.1)	65 (± 3.5)	61 (2.7)
Exchangeable cations			
Ca^{+}	17	12	6
Mg^{+}	2	3	1
Na^{+}	0.2	0.2	0.1
K^{+}	0.8	3	0.8
CEC cmol (+) kg^{-1}	20.6	19.1	9.2
BD (g cm^{-3})	1.4	1.3	1.3
Dominant clay mineralogy[a]	1:1 Smectite (23%)	2:1 Kaolinite (40%)	1:1 Smectite (20%)

Soil texture defined according to USDA soil textural triangle (Soil Survey Division Staff 1993)

POM particulate organic matter, *SA* sand and aggregate associated C, *SC* silt and clay associated C

[a]Detailed soil mineralogy data available in the supplementary material

of soil texture and mineralogy on SOM and GHG fluxes with 3 soil types (CLAY, LOAM, SAND) and 4 replicates. Factor 2 examined the effect of residue placement on SOM formation and GHG fluxes, with residue either being incorporated with the topsoil (MIX) or placed on the soil surface (SUR) on all three soils (CLAY, LOAM, SAND). In order to incorporate the residue with the soil for the MIX treatment, the surface 10 cm of soil was removed and placed in a plastic bag where the soil was manually broken apart into large macroaggregates (~ 1–2 cm in diameter). The labelled residue was then added to the soil and mixed to ensure an even distribution before being returned to the PVC tube. Two Controls were established; (1) no residue added, (2) no residue added but soil disrupted to a depth of 10 cm as in MIX treatment.

Residue and soil collection

At 12 months, all recognisable residue on the soil surface (not applicable to MIX treatment) was carefully removed by hand, dried at 60 °C, weighed and pulverized for further analyses. All soil cores (depth 10 cm) were excavated intact, placed in pre-labelled plastic bags and kept refrigerated (4 °C). Soil was sampled to a depth of 30 cm (therefore soil samples were taken 20 cm below the core extraction site). Soil (0–10 cm) were sieved to 2 mm prior to fractionation. Any organic matter > 2 mm in 0–10 cm layer was removed and analysed as part of the litter fraction (i.e. residue remaining on the soil surface in SUR and within the soil profile for MIX). Bulk soil analyses was conducted on 10–30 cm depth. A representative subsample from each soil sample was dried in an

oven at 60 °C, pulverised and used for elemental and isotopic analyses.

Soil (0–10 cm) was physically fractionated by size and density to obtain SOM components that were fundamentally different in terms on their formation, persistence, and functioning. We obtained (1) a light particulate organic matter (POM) fraction, which was comprised primarily of identifiable plant material that is chemically similar to its source and characterised by a relatively short turnover time as it is not protected within the mineral soil, (2) a sand-sized fraction (> 53 µm), which also contains OM physically protected within microaggregates, and (3) a silt and clay sized (< 53 µm) fraction where OM is physical-chemically associated with mineral surfaces. Fractions (2) and (3) are collectively referred to as mineral-associated organic matter (MAOM).

Briefly, 30 g of soil (< 2 mm) were added to 150 ml water and dispersed using a weak ultrasonic treatment (output energy of 22 J ml^{-1}) to disrupt macro aggregates, leaving more stable microaggregates intact (Amelung and Zech 1999). Low energy sonication should also act to preserve fragile particulate organic matter (POM) from artificial spreading within the size fractions (Stemmer et al. 1999). The dispersed suspension was then wet sieved over a 53 µm aperture sieve until the rinsing water was clear. The fraction > 53 µm, containing the sand and microaggregates (SA) together with POM, was dried at 40 °C and weighed. The suspension < 53 µm was filtered through a 0.45 µm aperture nylon mesh and the material > 0.45 µm (silt and clay fraction, SC) was dried at 40 °C and weighed. The filtrate (< 0.45 µm) containing soluble organic carbon was not directly measured, but was estimated as the difference between total ^{13}C content in the bulk soil and the sum of ^{13}C recovered in the three measured soil fractions (POM, SA, SC). Particulate organic matter was isolated by stirring the fraction > 53 µm with sodium polytungstate (SPT) at a density of 1.8 g cm^{-3}. The mixture was centrifuged at $1000 \times g$ for 15 min and the light fraction (POM) was decanted, washed with deionised water to remove all SPT, dried at 40 °C and weighed. All fractions were pulverized and analysed for C and N elemental and isotopic concentrations by EA-IRMS, as described above for the residue.

Clay mineralogy was determined by X-ray diffraction of oriented samples of bulk soil (ARL, EQUINOX 100). Quantitative analysis (percent mineralogy of bulk soil) was determined using the mineral intensity factors (MIF) in combination with the 100% approach (Moore and Reynolds Jr 1989). On the supposition that all phases present in the sample have been identified and that the sum of all phases is 100%, the proportional weight of each phase can be calculated using equation:

$$W_{\propto} = (I_{\propto} / \ \mathrm{MIF}_{\propto}) / \sum (I_n / \ \mathrm{MIF}_{\mathrm{n}})$$

where $I_{\propto}$ is the intensity of a selected peak from phase $\propto$ in the mixture, $\mathrm{MIF}_{\propto}$ the mineral intensity factor for phase $\propto$, $I_n$the intensity of a selected peak from any phase n in the mixture and $\mathrm{MIF}_{\mathrm{n}}$ the mineral intensity factor for phase n (Kahle et al. 2002).

GHG sampling and isotopic analyses

Soil CO_2 efflux measurements were carried out on a weekly basis for one year from February 2014 to February 2015. Measurements were taken using a portable soil CO_2 flux system (LI-COR 8200, LI-COR, Lincoln, Nebraska, USA). CO_2 flux rates were calculated using the instrument's software (LI-COR Viewer 1.3.0) from the linear increase in CO_2 concentration over time (chamber closure period of 2 min). For N_2O and CH_4 fluxes, gas samples were also taken using the static closed chamber approach (Parkin and Venterea 2010). Manual gas sampling was carried out weekly and within 24 h of the cessation of heavy rain events to try and ensure peak N_2O fluxes were captured.

For each measurement, an airtight PVC lid was placed on the collar and a sample drawn from the chamber headspace (5 cm) through a septum in the lid after 30 and 60 min. Samples were immediately injected into previously evacuated glass vials (12 ml) (Exetainer, Labco, High Wycombe, Buckinghamshire, UK) with a double wadded Teflon/silica and rubber septa. Gas samples were analysed for absolute concentration of N_2O and CH_4 using a gas chromatograph equipped with an ECD detector for N_2O and a FID for CH_4 (Agilent 7890A). Flux rates of N_2O and CH_4 were calculated from the slope of the linear increase in gas concentration during the closure period as described by Scheer et al. (2014). The coefficient of determination (r^2) was used as a quality check for linearity and flux rates were discarded if r^2 was < 0.85

for N_2O and CH_4. In order to calculate the $\delta^{13}C$ of the respired CO_2, gas samples were analysed for $^{13}CO_2$ using an IRMS linked to a Cryoprep trace gas concentration system (Sercon Limited 20–20, UK).

Data analyses

The residue-derived C and N contribution to the bulk soil, SOM fractions and CO_2 fluxes was assessed using the isotopic mixing model (Subke et al. 2004):

$$f_{residue} = (\delta_s - \delta_{control})/(\delta_{residue} - \delta_{control})$$

where $f_{residue}$ is the fraction of the residue-derived C contributing to the bulk soil, SOM fractions and CO_2. The δ_S and $\delta_{control}$ are the $\delta^{13}C$ of the specific bulk soil, SOM, or gas sample from the residue (δ_S) and the Control $(\delta_{control})$ treatment respectively. For bulk soil and SOM fractions, the $\delta_{control}$ average values across all Control plots are used. The $\delta_{residue}$ is the $\delta^{13}C$ of the initial residue.

The amount of residue-derived C in these pools were obtained by multiplying the $f_{residue}$ values to corresponding C pools or fluxes. Residue-derived C pools in the SOM fractions were calculated for the 0–10 cm soil depth by summing the respective 0–5 and 5–10 cm pool sizes. Soil-derived C fluxes were determined as the difference between total C flux and residue-derived C flux.

Daily soil CO_2 fluxes were determined from weekly measurements using a linear interpolation following Ngao et al. (2005). Daily N_2O fluxes were determined by linear interpolation between weekly sampling points, except for the days directly following a major emission pulse when an exponential decay curve was applied. The decay curve was calculated based on high resolution (hourly) N_2O flux data from a different experimental site, but using the same experimental set up in the same climatic zone (Mitchell et al. 2016).

SOC formation was measured as the amount of 'new' (added) ^{13}C left in the SOC pool after one year of in situ decomposition (all fractions). SOC stabilisation was measured as the amount of new (added) C recovered in the mineral-associated pools (SA and SC), collectively referred to as MAOM, after one year of in situ decomposition. The priming effect was calculated as the difference between soil-derived CO_2 flux in treatment and Control (no residue added). In order to calculate the overall GHG balance we used the IPCC (IPCC 2013) global warming potentials (GWP) factors over a 100 year time horizon to calculate CO_2-equivalents (CO_2 e) ha^{-1} $year^{-1}$ for the estimated balance between (1) SOC formation (all fractions), (2) treatment induced priming of soil C, and (3) treatment induced N_2O and CH_4 fluxes, using the following equations (Six et al. 2004):

$$SOC_{formation(all\,fractions;\,POM,SA,SC)} = SOC_{(all\,fractions)} \cdot \frac{44}{12} \cdot (-1)$$

$$SOC_{primed} = \left(CO_{2(soil-derived\,C\,flux\,treatment)} - CO_{2(soil-derived\,C\,flux\,control)}\right) \cdot \frac{44}{12}$$

$$N_2O = \left(N_2O_{(total\,flux\,treatment)} - N_2O_{(total\,flux\,control)}\right) \cdot 298$$

$$CH_4 = \left(CH_{4(total\,flux\,treatment)} - CH_{4(total\,flux\,control)}\right) \cdot 34$$

The overall GHG balance was calculated using the equation:

$$GHG\,balance = SOC\,formation + SOC\,primed + N_2O + CH_4$$

Only primed CO_2 was considered in the GHG balance (omitting residue-derived $^{13}CO_2$) as added residue C was considered as previously sequestered in plant material. Therefore, for the balance, only the additional decomposition of existing SOC generated by the input of plant residue was used in GHG accounting. Negative C priming (i.e. soil-derived C flux was greater in the control treatment) was not considered in the overall GHG balance as C inputs did not contribute to additional C loss. To combine uncertainties for the GHG balance calculation, we converted the individual variances into CO_2 equivalents and summed those values using the equation:

$$Var\,GHG\,balance = Var(SOC) + Var(SOC\,primed) + Var(N_2O) + Var(CH_4).$$

The square root of this sum is the estimated standard deviation. This computation of uncertainty implicitly assumes that the three components of total GWP are uncorrelated (Six et al. 2004).

A two-way ANOVA was conducted to examine the effects of factors (1) soil texture (CLAY, LOAM, SAND), and (2) residue placement (SUR, MIX) and their interaction on dependent variables: ((C located in

different SOC fractions: POM, SA, SC) and GHG fluxes (CO_2, N_2O and CH_4)). Residual analysis was performed to test for the assumptions of the two-way ANOVA. Normality was assessed using Shapiro–Wilk's normality test for each cell of design and homogeneity of variances was assessed by Levene's test. Where the assumption of homogeneity of variances was violated, data was transformed using the weighted least squares regression approach. The *P* and F values are indicated for significant variance in means across different factors (soil texture and residue placement) (significance, $P < 0.05$). A Tukey's post-hoc test was used for pairwise comparisons of means between each group (significance, $P < 0.05$).

Results

Soil properties

The three soils of the study site were chosen due to their variable physicochemical properties (Table 1). The soils were named according to their field texture, with a silty clay loam (CLAY), loam (LOAM) and a sandy loam (SAND). CLAY had the greatest clay content (49%) in comparison to LOAM (31%) and SAND (30%). Although the LOAM and SAND had a similar clay content, the SAND soil contained a higher proportion of coarse sand (LOAM = 9%, SAND = 16%), and half as much silt. The LOAM and SAND soils also differed significantly in (1) initial C and N content (LOAM C = 3.3%, N = 0.35% in comparison to SAND, C = 1.9% and N = 0.19% and (2) their mineralogy, with the LOAM soil containing a significantly higher proportion of kaolinite (1:1) clay minerals ($\sim$ 40%) in comparison to SAND, where the dominant clay mineralogy was smectite ($\sim$ 20%) (Supplementary material). CLAY had the highest proportion of C in the silt and clay fraction (81% of TOC) and the lowest proportion of C in the POM fraction (15% of TOC). In contrast the SAND soil had highest proportion of TOC in the POM fraction (36% of TOC) versus 61% in the SC fraction (Table 1).

Residue-derived C recovery

In CLAY there was a significantly greater decomposition of surface residues (in comparison to LOAM and SAND) that resulted in; (1) a significantly lower recovery of residue on the soil surface in CLAY, 35% ($\pm$ 3.9) compared to 51% ($\pm$ 5.5) in LOAM and 57% ($\pm$ 7.2) in SAND, (2) a significantly higher recovery of residue-derived SOC (CLAY = 7.6% $\pm$ 0.5, LOAM = 3.3% $\pm$ 0.4, SAND = 2.8% $\pm$ 0.4, and (3) a significantly greater residue-derived CO_2 flux (CLAY = 48% $\pm$ 3.9, LOAM = 32% $\pm$ 4.5 and SAND = 29% $\pm$ 2.8) (Fig. 1). The MIX treatment resulted in significantly lower recovery of undecomposed residue with an average of 33% ($\pm$ 4.2) of residue remaining in the soil (> 2 mm), compared to an average of 48% ($\pm$ 5.2) in surface applied treatments. MIX also resulted in a significant increase in residue-derived CO_2 flux and a four to five-fold increase in the amount of residue-derived SOC, in comparison to SUR treatments.

C priming and GHG fluxes

The cumulative CO_2 flux was partitioned into native SOC-derived CO_2 and residue-derived CO_2 using the ^{13}C tracer method (Fig. 2). In general, the greatest residue-derived CO_2 fluxes occurred in CLAY when residue was incorporated with the topsoil (MIX) and these factors were compounded by (1) warm and wet summer conditions (February to May 2014) and (2) the time elapsed since residue application as the greatest fluxes followed fresh residue application in February 2014 (Fig. 3).

CLAY experienced a significant positive priming effect over 12 months (i.e. soil-derived CO_2 flux > CO_2 flux control) (Fig. 2) (Table 2), particularly in the SUR treatment where it increased the soil-derived CO_2 flux by $\sim$ 10% (indicated by letter (A) in Fig. 2). The magnitude of the priming effect in CLAY SUR was almost double SOC accrual over the same 12 month period (total SOC accrual = 2405 kg CO_2 e ha^{-1}, total CO_2 primed = 4174 kg CO_2 e ha^{-1}) (Table 3) meaning that SOC accrual was completely offset by C priming. There was also a positive C priming effect in CLAY MIX (indicated by letter (B) in Fig. 2), but this was not of a sufficient magnitude to offset SOC gains (Table 3). The incorporation of residue (MIX) significantly reduced the priming effect across all soil types. There was a significant interaction between soil type and residue placement whereby residue incorporation significantly increased C priming in CLAY, but resulted in a significant decrease in C priming in SAND (Tables 2, 3).

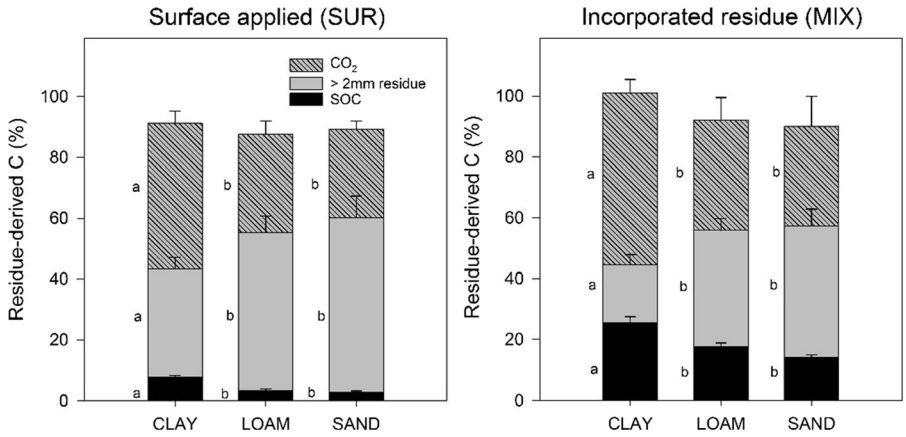

Fig. 1 Residue-derived C recovery in different compartments in 3 soil types (CLAY, LOAM, SAND) for the surface applied treatment (SUR) and the incorporation treatment (MIX) after 365 days of in situ decomposition 0–30 cm. C compartments: (1) residue-derived CO_2 (2) undecomposed residue on soil surface and coarse organic matter (> 2 mm) in soil, and (3) residue-derived SOC (< 2 mm). Averages with standard errors are reported (n = 4). Letters indicate significance ($p < 0.05$) between soil types via analysis of variance (ANOVA)

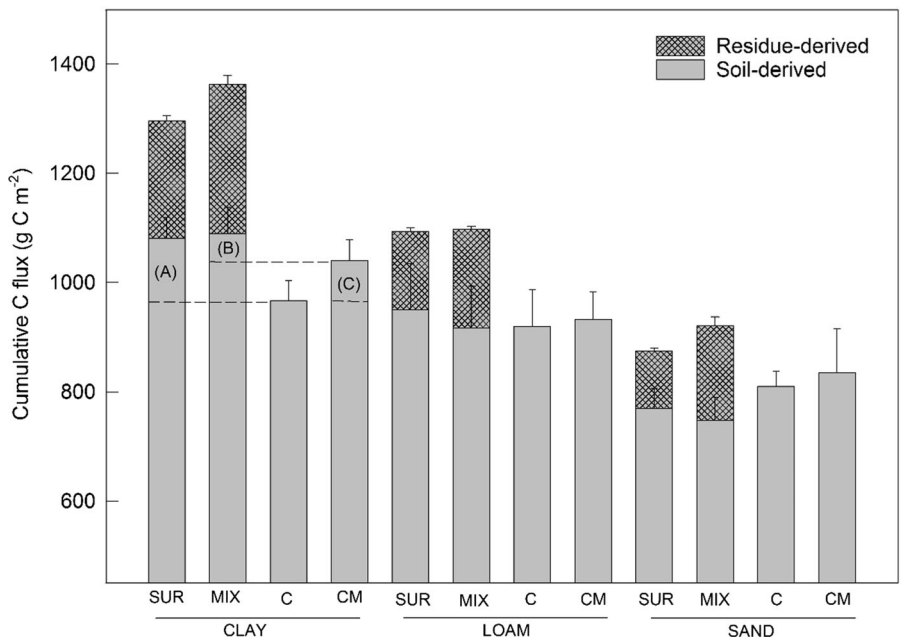

Fig. 2 Cumulative residue and soil-derived CO_2 flux for three soil types (CLAY, LOAM, SAND) and placement (SUR, MIX) over 12 months of in situ decomposition. C = control, CM = control mix. **a** Significant C priming effect ($p < 0.05$) in CLAY SUR treatment (i.e. the difference between soil-derived CO_2 flux and Control). **b** Significant priming effect in CLAY MIX (i.e. the difference between soil-derived CO_2 flux and control mix. **c** indicates the difference in CO_2 flux between control (no residue applied, no soil mixing) and control mix (no residue applied and soil mixed/ disrupted to a depth of 10 cm). Therefore (**c**) indicates the difference in C mineralisation with the disturbance of soil. Averages with standard errors are reported (n = 4)

The greatest N_2O fluxes coincided with large rainfall events, resulting in two major N_2O emission pulses (Fig. 3). The first emission pulse, recorded one day after a significant rainfall event (105 mm, 28 March 2014), resulted in N_2O fluxes representing ~ 50% of annual emissions. Soil texture, but

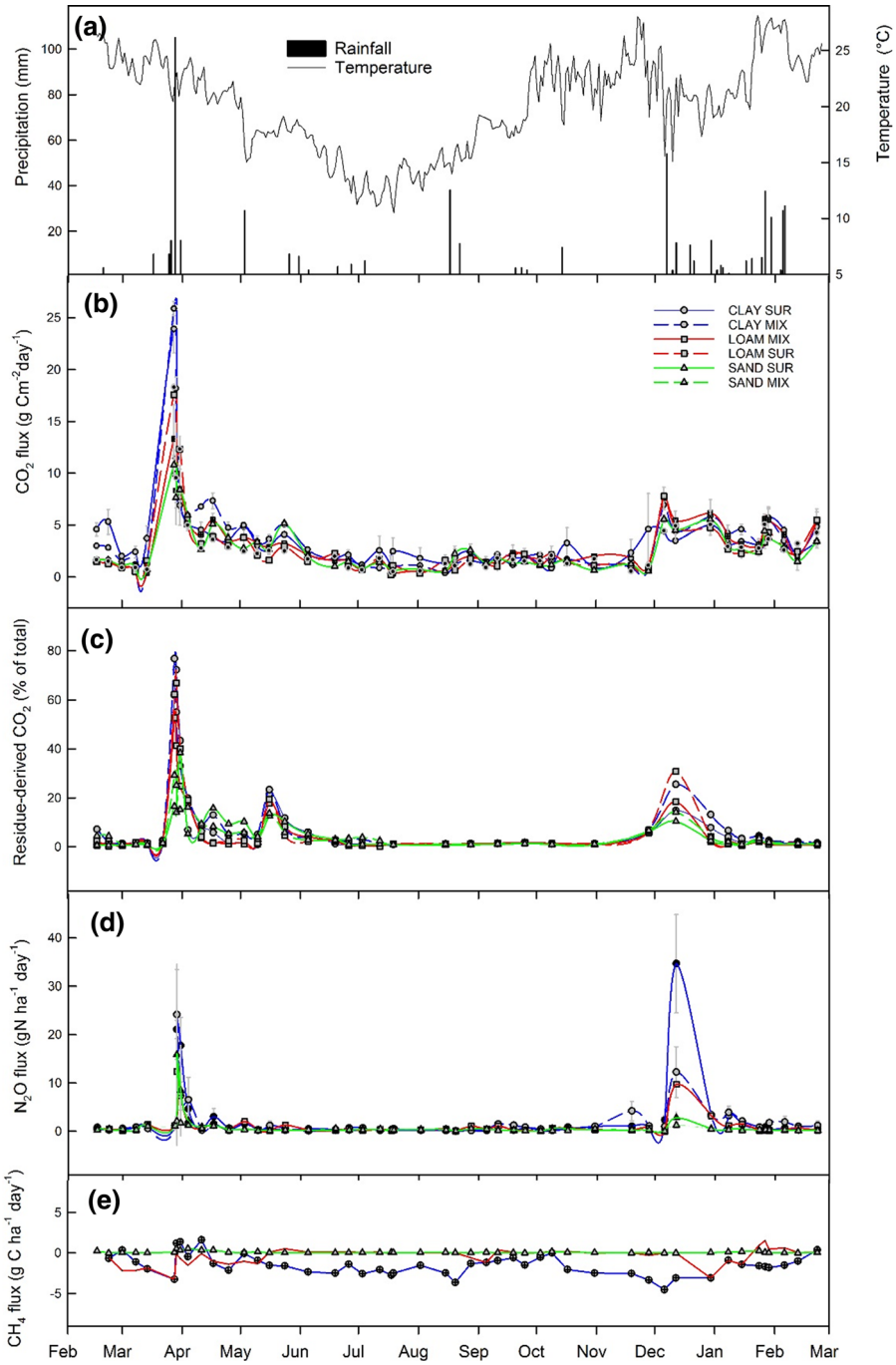

Fig. 3 **a** Rainfall and temperature during the study period (February 2014- February 2015); **b** temporal dynamics for CO_2; **c** residue-derived CO_2 flux (% contribution to total CO_2 flux); **d** temporal dynamics for N_2O; and **e** temporal dynamics for CH_4. GHG dynamics are shown for 3 soil types (CLAY, LOAM, SAND) and 2 treatments (surface applied residue = SUR and incorporated residue = MIX). Average value of SUR and MIX are shown for CH_4 as residue incorporation had no significant effect on CH_4 flux

Table 2 A two-way ANOVA was used to determine the statistical significance of the effect of factors (1) soil type (CLAY, LOAM, SAND) and (2) placement of residue (surface applied, SUR and incorporated, MIX), and their interaction, on dependent variables

Dependent variable	Soil type (CLAY, LOAM, SAND). Letters indicate Tukey's post-hoc	Residue incorporation (MIX, SUR). Letters indicate Tukey's post-hoc	Soil type x residue incorporation
CO_2-C	$P = < 0.01$, F = 12.9	$P = 0.425$, F = 0.68	$P = 0.994$, F = 0.06
	CLAY^a LOAM^b SAND^b	MIX^a SUR^a	
Residue $^{13}CO_2$	$P = < 0.01$, F = 121.9	$P = 0.03$, F = 5.9	P = 0.07, F 0.5
	CLAY^a LAOM^b SAND^b	MIX^a SUR^b	
CO_2 (primed)	$P = < 0.001$, F = 219.1	$P = 0.05$, F = 7.2	P = < 0.001 (see (*) for explanation)
	CLAY^a LOAM^b SAND^b	MIX^a SUR^b	
^{13}C POM	$P = < 0.001$, F = 9.5	$P = 0.01$, F = 8.3	$P = 0.72$, F = 0.334
	CLAY^a LOAM^b SAND^b	MIX^a SUR^b	
^{13}C SA	$P = 0.01$, F = 9.9	$P = < 0.001$, F = 26.7	$P = 0.814$, F = 0.2
	CLAY^a LOAM^b SAND^b	MIX^a SUR^b	
^{13}C SC	$P = 0.05$, F = 4.89	$P = 0.03$, F = 5.3	$P = 0.89$, F = 0.11
	CLAY^a LOAM^b SAND^c	MIX^a SUR^b	
N_2O-N	$P = 0.04$, F = 8.73	$P = 0.754$, F = 0.13	$P = 0.43$, F = 0.883
	CLAY^a LOAM^b SAND^b	MIX^a SUR^a	
CH_4	$P \leq 0.001$, F = 19.2	$P = 0.516$, F = 0.448	$P = 0.731$, F = 0.332
	CLAY^a LOAM^b SAND^b	MIX^a SUR^a	

P and F values are reported with letters indicating post-hoc Tukey's test applied for statistical difference between soil types (CLAY, LOAM, SAND)

13C isotopically enriched applied residue, *POM* particulate organic matter, *SA* sand and aggregate associated organic carbon, *SC* silt and clay associated organic carbon

*CO_2 primed increased with clay content (CLAY > LOAM > SAND) and significantly decreased with residue incorporation (MIX) and there was a significant interaction: Residue incorporation (MIX) significantly increased C priming in CLAY but significantly decreased C priming in SAND, with no significant effect on C priming in LOAM

Table 3 The overall GHG balance over 12 months showing the balance between SOC gain (in all fractions, POM, SA, SC) versus GHG losses from C priming, N_2O and CH_4 all expressed in CO_2 equivalents (kg CO_2e ha^{-1})

Soil type	Residue placement	SOC accrual (all fractions)	CO_2 priming	N_2O	CH_4	GHG balance
CLAY	SUR	− 2405	4174	193	− 0.80	*+ 1961 (± 368)*
	MIX	− 9330	1833	231	− 0.92	**− 7267 (± 414)**
LOAM	SUR	− 1225	1082	18	− 0.09	**− 124 (± 398**
	MIX	− 6467	(− 534)	85	− 0.08	**− 6382 (± 579)**
SAND	SUR	− 1031	(− 1471)	16	− 0.23	**− 1015 (± 433)**
	MIX	− 5165	(− 3200)	15	− 0.08	**− 5150 (± 357)**

Overall GHG balance is expressed in (kg CO_2e ha^{-1}) with a net positive balance in italic and net negative balance in bold

not mixing, had a significant impact on N_2O emissions with a doubling of N_2O flux between each soil type (CLAY = 1445 kg N_2O-N ha^{-1}, LOAM = 682 kg N_2O-N ha^{-1}, SAND = 322 kg N_2O-N ha^{-1}). There was a significantly greater uptake of CH_4 in CLAY (0.69 kg CH_4-C ha^{-1}) soil versus LOAM and SAND (average of 0.09 kg CH_4-C ha^{-1}) (Fig. 3, Table 2), with no effect of residue incorporation.

Residue-derived SOC formation and stabilisation

Soil texture and the incorporation of residue were both significant in accounting for the conversion of residue-C inputs to SOC, with the greatest residue-derived C content in CLAY when residue was incorporated (MIX) (Fig. 4, Table 2). The incorporation of residue (MIX) significantly increased the conversion of residue inputs to SOC in all fractions (POM, SA and SC), resulting in a fourfold increase in residue-POM, a threefold increase in residue-SA, and a 2.5-fold increase in residue-SC (Fig. 4). CLAY contained a significantly greater amount of residue-derived SOC in all fractions, in comparison to LOAM and SAND. There was no significant difference in residue-derived C recovery between LOAM and SAND, except in the SC fraction, where there was a significantly greater residue-derived C content in SC fraction in SAND.

Overall GHG balance

In order to gain an understanding of the balance between residue inputs and resulting GHG losses (primed CO_2 and treatment-induced N_2O, and CH_4 flux) all values were converted to CO_2 equivalents (CO_2 e ha^{-1}) (Table 3). Overall, residue incorporation (MIX) resulted in a greater net GHG sink—meaning SOC accrual was greater than GHG fluxes over a 12 month period. In. CLAY SUR, SOC accrual was offset by greater GHG losses, primarily due to large native SOC-priming losses, resulting in a net GHG source over 12 months (+ 1961 kg CO_2 ha^{-1}). Although N_2O losses increased with residue addition (∼ twofold increase across all treatments), their magnitude had only a small influence on the overall GHG balance. CH_4 uptake was significantly greater in CLAY, but again the influence on GHG balance was minimal.

Discussion

Results reveal a trade-off in the initial stages of residue decomposition between increasing 'new' SOC formation, whilst simultaneously increasing the vulnerability of native SOC stocks by C priming as determined by soil properties and residue placement. This has important implications for climate change mitigation strategies aimed at increasing SOC stocks by increasing biomass inputs.

Greater decomposition in CLAY (as shown by greater native soil-derived CO_2 and residue-derived $^{13}CO_2$) is in contrast to the conventional concept that soils with a higher clay content reduce SOC turnover due to the protection of SOM from microbial decomposition by mineral surfaces (Burke et al. 1989; Hassink 1997; Six et al. 2002). We speculate that CLAY promoted a greater degree of decomposition due to a more favourable environment for microbial decomposition by supporting higher moisture retention (and greater water conductivity from lower soil layers) than LOAM or SAND (Fissore et al. 2016; Singh et al. 2017; Thomsen et al. 2003). In contrast, a lower amount of decomposition in the SAND soil was likely due a lack of moisture retention as a function of texture, limiting the diffusion of enzymes and

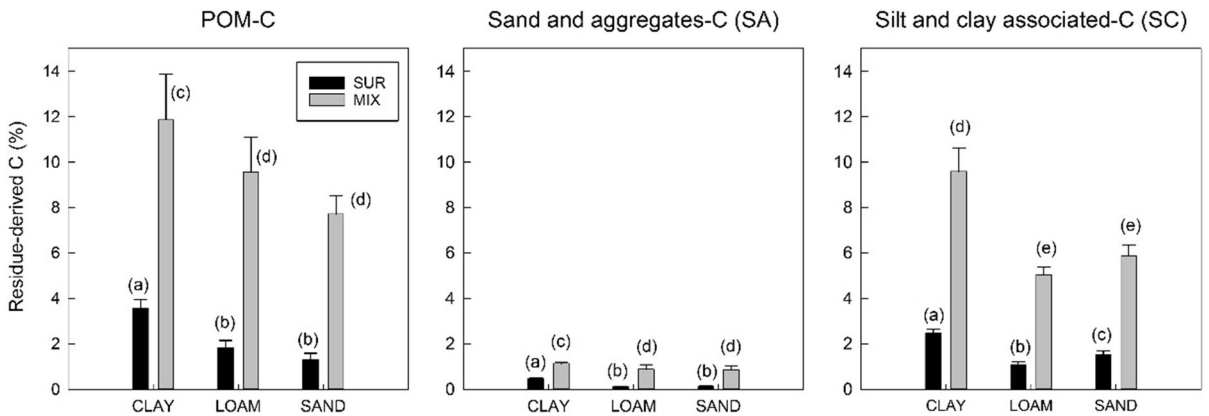

Fig. 4 ^{13}C recovery in SOC fractions. Particulate organic matter (POM), sand and aggregate associated organic carbon (SA), silt and clay associated carbon (SC) 0–10 cm. Letters indicate statistical significance ($p < 0.05$) across soil type using ANOVA

substrate during the prolonged dry winter periods (Chivenge et al. 2011; Gentile et al. 2008; Strong et al. 2004).

A greater amount of residue decomposition in CLAY corresponded to a greater formation of new 'protected' residue-derived SOC (1) entrapped within microaggregates (SA) and, (2) in close contact with mineral surfaces (SC)—referred to collectively as MAOM. A greater proportion of MAOM accrual in CLAY was promoted due to the reactivity of clay-sized minerals, which allowed organic and mineral particles to adhere together to form micro-structured clay and silt-sized compound particles (Chorover et al. 2004). These compound particles then act as composite building units of MAOM (Chenu and Stotzky 2002; Kögel-Knabner et al. 2008; Lehmann et al. 2007). CLAY also promoted the formation of microaggregates through a greater microbial growth and activity with the by-products of metabolism being important in microaggregate adhesion (Chenu 1989; Oades 1993; Six et al. 2002).

Whilst soil texture was significant in stabilising a greater amount of residue-derived SOC in the CLAY soil, it only partially explains why 'new' SOC content in MAOM was significantly greater in SAND *versus* LOAM, given their similar clay content (SAND = 31%, LOAM = 30%). The most likely explanation for this is due to variations in soil properties and specific characteristics of the mineral phase of each soil. XRD results confirmed that the LOAM soil was dominated by 1:1 kaolinite clay mineral ($\sim$ 40%) which has a lower surface area and charge density (in comparison to the smectite-dominated CLAY and SAND soils) and consequently of less protective of necromass and metabolite C released during the decomposition process (Saggar et al. 1996; Torn et al. 1997).

The incorporation of residue (MIX) was also significant in the conversion of residue inputs to SOC (all fractions) indicating the greater efficiency of the below-ground pathway for SOC formation. Whilst the effect of animal trampling on residue incorporation is still debated (e.g. Carter et al. 2014; Savory and Butterfield 1998), a higher SOC formation from the belowground residue inputs indicates that grasslands have a high potential for C sequestration from increased forage production as they allocate a significant proportion of their photosynthate belowground (Silver et al. 2010). Greater SOC formation from incorporated residue was likely due to the closer proximity of residue to stabilising mineral surfaces and increased accessibility of microbes to residue-derived C as a function of placement (Helgason et al. 2014). Therefore the incorporation of residue likely promotes a microbial habitat analogous to the rhizosphere by enhancing the probability of 'new' plant C substrate assimilation by microbes (Sokol et al. 2018) with microbial by-products subsequently forming chemical association with proximate mineral surfaces. Furthermore, a more favourable microclimate for decomposition likely occurred at depth (Beare et al. 1992), whilst the disruption of the soil structure by mixing promoted soil aeration.

A greater SOC formation (all fractions) in CLAY SUR was completely outweighed by the priming of 'old' or native SOC resulting in a net C loss. The priming effect increased CO_2 flux by $\sim$ 10% which is at the lower end of an average of 37% increase reported by Luo et al. (2016) and is contrary to numerous studies reporting lower priming effects in finer textured soils due to protection of OM by mineral surfaces (e.g. Fang et al. 2018). Although the mechanisms explaining a greater C priming effect in CLAY cannot be fully elucidated, we speculate that greater priming occurred due to a higher moisture content in CLAY which facilitated decomposition and the release of labile-C inputs, which prompted a greater growth and activity of microbial biomass. This alleviated the spatial inaccessibility of microbes to native SOC, resulting in the decomposition of both residue-C and native C (co-metabolism) (Bell et al. 2003; Kuzyakov and Bol 2006; Shahbaz et al. 2017). It cannot be determined whether native SOC was mineral-bound (MAOM) or free-light non-mineral associated (POM). However, given that 85% of native SOC was MAOM in CLAY, we suggest that a portion of this was mobilised via abiotic reactions, for example chemical desorption, that may have been promoted via a higher moisture content in CLAY (Huang and Hall 2017). The smectite-rich CLAY soil may have also been subject to a greater degree of shrinking and swelling, exposing previously occluded C to microbial attack (Smucker et al. 2007).

The incorporation of residue acted to significantly reduce the magnitude of the priming effect. This was presumably due to the preferential utilisation of labile fresh residue input which limited microbial requirement to access nutrients and energy in native SOM

(Guenet et al. 2010; Kuzyakov 2000). A positive priming effect still occurred in CLAY MIX despite the likely antagonistic effect of mixing exposing 'new' native SOM surfaces to microbial attack through aggregate disruption and improved soil aeration (Beare et al. 1994; Beyaert and Paul Voroney 2011; Burgess et al. 2002). A reduction in the priming of native SOC due to the incorporation of residue highlights the need to further understand the interactions between fresh residue inputs and native SOC in the context if restoring soil fertility and sequestering C.

Soil physical properties significantly impacted the emission of CH_4 and N_2O; however, the magnitude of these losses was minor in comparison to C priming losses (as shown when values were converted to CO_2 equivalents). The addition of a high-quality residue to the soil (C: N ratio 13:1) containing labile C and organic N greatly increased N_2O fluxes associated with the processes of nitrification and denitrification. The greatest N_2O fluxes occurred in CLAY directly after heavy rainfall events suggesting the main N_2O loss pathway was denitrification under anaerobic conditions, which has been demonstrated as a major N loss pathway in subtropical grassland soils (Rowlings et al. 2015). Therefore the impact of soil texture on N_2O emissions was most likely indirect through O_2 availability because soil texture can substantially shape the size and distribution of soil pores and therefore influence soil aeration and water content (Singurindy et al. 2006). A lower CH_4 uptake in the coarser textured soils (LOAM and SAND) was likely due to lower soil moisture content limiting methanotrophic activity (van Delden et al. 2018).

The timeframe of the experiment (limited to 12 months) and the different temporal responses of C stores and fluxes must be considered in this analysis. For example, in the SUR treatment, a large proportion of residue remained undecomposed on the soil surface (35–57%), with no certainty on its fate beyond the timeframe of the experiment. We hypothesise that this remaining residue cannot continue to accrue within MAOM indefinitely as it is likely that MAOM will begin to reach a point of saturation (Castellano et al. 2015; Six et al. 2002; Stewart et al. 2007) as demonstrated over 12 months of decomposition in Mitchell et al. (2016). Therefore, additional C inputs from further decomposition beyond 12 months will likely increasingly accumulate in more labile fractions (i.e. POM), which is readily accessed by microbes and lost from the system as CO_2. Whilst SOC may reach saturation, elevated N_2O or CH_4 emissions (C priming not considered as demonstrated to act for a short period) can persist on longer timescales, meaning that early benefits from SOC gain can be increasingly offset by other emissions.

In conclusion, a trade-off exists in the short-term between 'new' SOC stabilisation through increased C inputs and increased GHG losses (in particular priming of 'old' C), as controlled by soil texture and residue placement. In finer textured soils, SOC accrual was significantly outweighed by GHG losses (expressed in CO_2 equivalents), primarily from 'old' native SOC priming. This GHG balance was improved through the incorporation of residue, which acted to (1) increase residue-derived SOC formation by 4- to 5-fold and (2) reduce C-priming losses presumably due to greater access to fresh C substrate. Increasing C inputs can result in net C loss in the short-term, particularly in finer textured soils, highlighting the need for soil assessments prior to the implementation of any soil-based mitigation measures that increase biomass inputs.

Acknowledgements The project was financially supported by the Australian Government's Department of Agriculture, and Water Resources as part of the National Soil Carbon Programme (Filling the Research Gap, FtRG) (project number 01203.073). The data reported in this paper were obtained at the Central Analytical Research Facility (CARF) operated by the Institute of Future Environments (QUT). We would like to thank Johannes Friedl and Rene Diocares for their work on IR-MS; Sarah Carrick for her work on soil fractionation; and Robert Rowlings for access to the site and data collection. Access to CARF is supported by generous funding from the Science and Engineering Faculty (QUT).

References

Amelung W, Zech W (1999) Minimisation of organic matter disruption during particle-size fractionation of grassland epipedons. Geoderma 92:73–85

Asner GP, Elmore AJ, Olander LP, Martin RE, Harris AT (2004) Grazing systems, ecosystem responses, and global change. Annu Rev Environ Resour 29:261–299

Azam F, Müller C, Weiske A, Benckiser G, Ottow J (2002) Nitrification and denitrification as sources of atmospheric nitrous oxide–role of oxidizable carbon and applied nitrogen. Biol Fertil Soils 35:54–61

Beare MH, Parmelee RW, Hendrix PF, Cheng W, Coleman DC, Crossley D (1992) Microbial and faunal interactions and

effects on litter nitrogen and decomposition in agroecosystems. Ecol Monogr 62:569–591
Beare M, Hendrix P, Cabrera M, Coleman D (1994) Aggregate-protected and unprotected organic matter pools in conventional-and no-tillage soils. Soil Sci Soc Am J 58:787–795
Bell JM, Smith JL, Bailey VL, Bolton H (2003) Priming effect and C storage in semi-arid no-till spring crop rotations. Biol Fertil Soils 37:237–244
Beyaert R, Paul Voroney R (2011) Estimation of decay constants for crop residues measured over 15 years in conventional and reduced tillage systems in a coarse-textured soil in southern Ontario. Can J Soil Sci 91:985–995
Burgess M, Mehuys G, Madramootoo C (2002) Nitrogen dynamics of decomposing corn residue components under three tillage systems. Soil Sci Soc Am J 66:1350–1358
Burke IC, Yonker CM, Parton WJ, Cole CV, Schimel D, Flach K (1989) Texture, climate, and cultivation effects on soil organic matter content in US grassland soils. Soil Sci Soc Am J 53:800–805
Byrnes RC, Eastburn DJ, Tate KW, Roche LM (2018) A global meta-analysis of grazing impacts on soil health indicators. J Environ Qual 47:758
Carter J, Jones A, O'Brien M, Ratner J, Wuerthner G (2014) Holistic management: misinformation on the science of grazed ecosystems. Int J Biodivers 2014
Castellano MJ, Mueller KE, Olk DC, Sawyer JE, Six J (2015) Integrating plant litter quality, soil organic matter stabilization and the carbon saturation concept. Glob Change Biol 21:3200
Chenu C (1989) Influence of a fungal polysaccharide, scleroglucan, on clay microstructures. Soil Biol Biochem 21:299–305
Chenu C, Stotzky G (2002) Interactions between microorganisms and soil particles: an overview. Wiley, New York
Chivenge P, Vanlauwe B, Gentile R, Six J (2011) Organic resource quality influences short-term aggregate dynamics and soil organic carbon and nitrogen accumulation. Soil Biol Biochem 43:657–666
Chorover J, Amistadi MK, Chadwick OA (2004) Surface charge evolution of mineral-organic complexes during pedogenesis in Hawaiian basalt. Geochim Cosmochim Acta 68:4859–4876
Conant RT, Paustian K (2002) Potential soil carbon sequestration in overgrazed grassland ecosystems. Glob Biogeochem Cycles 16:90-1–90-9
Conant RT, Cerri CE, Osborne BB, Paustian K (2017) Grassland management impacts on soil carbon stocks: a new synthesis. Ecol Appl 27:662–668
Cotrufo MF, Wallenstein MD, Boot CM, Denef K, Paul E (2013) The Microbial Efficiency-Matrix Stabilization (MEMS) framework integrates plant litter decomposition with soil organic matter stabilization: do labile plant inputs form stable soil organic matter? Glob Change Biol 19:988–995
Derner J, Schuman G (2007) Carbon sequestration and rangelands: a synthesis of land management and precipitation effects. J Soil Water Conserv 62:77–85
Dungait JA, Hopkins DW, Gregory AS, Whitmore AP (2012) Soil organic matter turnover is governed by accessibility not recalcitrance. Glob Change Biol 18:1781–1796
Fang Y, Nazaries L, Singh BK, Singh BP (2018) Microbial mechanisms of carbon priming effects revealed during the interaction of crop residue and nutrient inputs in contrasting soils. Glob Change Biol 24:2775
Fissore C, Jurgensen MF, Pickens J, Miller C, Page-Dumroese D, Giardina CP (2016) Role of soil texture, clay mineralogy, location, and temperature in coarse wood decomposition—a mesocosm experiment. Ecosphere 7:e01605
Fontaine S, Bardoux G, Abbadie L, Mariotti A (2004) Carbon input to soil may decrease soil carbon content. Ecol Lett 7:314–320
Gentile R, Vanlauwe B, Chivenge P, Six J (2008) Interactive effects from combining fertilizer and organic residue inputs on nitrogen transformations. Soil Biol Biochem 40:2375–2384
Goldman MB, Groffman PM, Pouyat RV, McDonnell MJ, Pickett ST (1995) CH4 uptake and N availability in forest soils along an urban to rural gradient. Soil Biol Biochem 27:281–286
Guenet B, Neill C, Bardoux G, Abbadie L (2010) Is there a linear relationship between priming effect intensity and the amount of organic matter input? Appl Soil Ecol 46:436–442
Guo X, Drury CF, Yang X, Reynolds WD, Zhang R (2012) Impacts of wet–dry cycles and a range of constant water contents on carbon mineralization in soils under three cropping treatments. Soil Sci Soc Am J 76:485–493
Hassink J (1997) The capacity of soils to preserve organic C and N by their association with clay and silt particles. Plant Soil 191:77–87
Helgason B, Gregorich E, Janzen H, Ellert B, Lorenz N, Dick R (2014) Long-term microbial retention of residue C is site-specific and depends on residue placement. Soil Biol Biochem 68:231–240
Huang W, Hall SJ (2017) Elevated moisture stimulates carbon loss from mineral soils by releasing protected organic matter. Nat Commun 8:1–10
IPCC (2013). Fifth assessment report. climate change 2013: the physical science basis. . In: Intergovernmental panel on climate change. Geneva, Switzerland
Jenkinson D, Fox R, Rayner J (1985) Interactions between fertilizer nitrogen and soil nitrogen—the so-called 'priming'effect. J Soil Sci 36:425–444
Kahle M, Kleber M, Jahn R (2002) Review of XRD-based quantitative analyses of clay minerals in soils: the suitability of mineral intensity factors. Geoderma 109:191–205
Kaiser K, Kalbitz K (2012) Cycling downwards–dissolved organic matter in soils. Soil Biol Biochem 52:29–32
Kleber M, Eusterhues K, Keiluweit M, Mikutta C, Mikutta R, Nico PS (2015) Mineral–organic associations: formation, properties, and relevance in soil environments. In: Advances in agronomy, vol. 130. Elsevier, pp 1–140
Kögel-Knabner I, Guggenberger G, Kleber M, Kandeler E, Kalbitz K, Scheu S, Eusterhues K, Leinweber P (2008) Organo-mineral associations in temperate soils: Integrating biology, mineralogy, and organic matter chemistry. J Plant Nutr Soil Sci 171:61–82
Krull ES, Baldock JA, Skjemstad JO (2003) Importance of mechanisms and processes of the stabilisation of soil

organic matter for modelling carbon turnover. Funct Plant Biol 30:207–222
Kuzyakov (2000) Review of mechanisms and quantification of priming effects. Soil Biol Biochem 32:1485–1498
Kuzyakov Y, Bol R (2006) Sources and mechanisms of priming effect induced in two grassland soils amended with slurry and sugar. Soil Biol Biochem 38:747–758
Lavallee JM, Soong JL, Cotrufo MF (2019) Conceptualizing soil organic matter into particulate and mineral-associated forms to address global change in the 21st century. Glob Change Biol 26:261
Lehmann J, Kinyangi J, Solomon D (2007) Organic matter stabilization in soil microaggregates: implications from spatial heterogeneity of organic carbon contents and carbon forms. Biogeochemistry 85:45–57
Lipper L, Dutilly-Diane C, McCarthy N (2010) Supplying carbon sequestration from West African rangelands: opportunities and barriers. Rangel Ecol Manag 63:155–166
Luo Z, Wang E, Sun OJ (2016) A meta-analysis of the temporal dynamics of priming soil carbon decomposition by fresh carbon inputs across ecosystems. Soil Biol Biochem 101:96–103
Mitchell E, Scheer C, Rowlings DW, Conant RT, Cotrufo MF, van Delden L, Grace PR (2016) The influence of aboveground residue input and incorporation on GHG fluxes and stable SOM formation in a sandy soil. Soil Biol Biochem 101:104–113
Mitchell E, Scheer C, Rowlings D, Conant RT, Cotrufo MF, Grace P (2018) Amount and incorporation of plant residue inputs modify residue stabilisation dynamics in soil organic matter fractions. Agric Ecosyst Environ 256:82–91
Moore D, Reynolds Jr R (1989) X-ray diffraction and the identification and analysis of clay minerals. In: X-ray diffraction and the identification and analysis of clay minerals
Morgan JA, Follett RF, Allen LH, Del Grosso S, Derner JD, Dijkstra F, Franzluebbers A, Fry R, Paustian K, Schoeneberger MM (2010) Carbon sequestration in agricultural lands of the United States. J Soil Water Conserv 65:6A–13A
Morley N, Baggs E (2010) Carbon and oxygen controls on N2O and N2 production during nitrate reduction. Soil Biol Biochem 42:1864–1871
Ngao J, Epron D, Brechet C, Granier A (2005) Estimating the contribution of leaf litter decomposition to soil CO_2 efflux in a beech forest using ^{13}C-depleted litter. Glob Change Biol 11:1768–1776
Oades J (1993) The role of biology in the formation, stabilization and degradation of soil structure. Geoderma 56:377–400
Ohm H, Hamer U, Marschner B (2007) Priming effects in soil size fractions of a podzol Bs horizon after addition of fructose and alanine. J Plant Nutr Soil Sci 170:551–559
Parkin TB, Venterea RT (2010) USDA-ARS GRACEnet project protocols, chapter 3. Chamber-based trace gas flux measurements. In: Sampling protocols. Beltsville, MD, pp 1–39
Provenza FD (2008) Benefits of multi-paddock grazing management on rangelands: limitations of experimental grazing research and knowledge gaps
Rowlings D, Grace P, Scheer C, Liu S (2015) Rainfall variability drives interannual variation in N2O emissions from a humid, subtropical pasture. Sci Total Environ 512:8–18
Ryals R, Kaiser M, Torn MS, Berhe AA, Silver WL (2014) Impacts of organic matter amendments on carbon and nitrogen dynamics in grassland soils. Soil Biol Biochem 68:52–61
Saggar S, Parshotam A, Sparling G, Feltham C, Hart P (1996) ^{14}C-labelled ryegrass turnover and residence times in soils varying in clay content and mineralogy. Soil Biol Biochem 28:1677–1686
Sanjari G, Ghadiri H, Ciesiolka CA, Yu B (2008) Comparing the effects of continuous and time-controlled grazing systems on soil characteristics in Southeast Queensland. Soil Res 46:348–358
Savory A, Butterfield J (1998) Holistic management: a new framework for decision making. Island Press, Washington, DC
Sayre NF, McAllister RR, Bestelmeyer BT, Moritz M, Turner MD (2013) Earth stewardship of rangelands: coping with ecological, economic, and political marginality. Front Ecol Environ 11:348–354
Scheer C, Rowlings DW, Firrel M, Deuter P, Morris S, Grace PR (2014) Impact of nitrification inhibitor (DMPP) on soil nitrous oxide emissions from an intensive broccoli production system in sub-tropical Australia. Soil Biol Biochem 77:243–251
Schuman G, Reeder J, Manley J, Hart R, Manley W (1999) Impact of grazing management on the carbon and nitrogen balance of a mixed-grass rangeland. Ecol Appl 9:65–71
Shahbaz M, Kuzyakov Y, Heitkamp F (2017) Decrease of soil organic matter stabilization with increasing inputs: mechanisms and controls. Geoderma 304:76–82
Silver WL, Ryals R, Eviner V (2010) Soil carbon pools in California's annual grassland ecosystems. Rangel Ecol Manag 63:128–136
Singh M, Sarkar B, Biswas B, Bolan NS, Churchman GJ (2017) Relationship between soil clay mineralogy and carbon protection capacity as influenced by temperature and moisture. Soil Biol Biochem 109:95–106
Singurindy O, Richards BK, Molodovskaya M, Steenhuis TS (2006) Nitrous oxide and ammonia emissions from urine-treated soils. Vadose Zone J 5:1236–1245
Six J, Elliott E, Paustian K (1999) Aggregate and soil organic matter dynamics under conventional and no-tillage systems. Soil Sci Soc Am J 63:1350–1358
Six J, Conant R, Paul E, Paustian K (2002) Stabilization mechanisms of soil organic matter: implications for C-saturation of soils. Plant Soil 241:155–176
Six J, Ogle SM, Conant RT, Mosier AR, Paustian K (2004) The potential to mitigate global warming with no-tillage management is only realized when practised in the long term. Glob Change Biol 10:155–160
Smucker AJ, Park E-J, Dorner J, Horn R (2007) Soil micropore development and contributions to soluble carbon transport within macroaggregates. Vadose Zone J 6:282–290
Soil Survey Division Staff (1993) Soil Survey manual. Soil Conservation Service, U.S. Department of Agriculture Handbook, Chapter 3
Sokol N, Sanderman J, Bradford M (2018) Pathways of mineral soil carbon formation: integrating the role of plant carbon

source, chemistry, and point-of-entry. Glob Change Biol 25:12

Southorn N (2002) The soil structure component of soil quality under alternate grazing management strategies. Adv Geoecol 35:163–170

Stemmer M, Von Lützow M, Kandeler E, Pichlmayer F, Gerzabek M (1999) The effect of maize straw placement on mineralization of C and N in soil particle size fractions. Eur J Soil Sci 50:73–85

Stewart C, Paustian K, Conant R, Plante A, Six J (2007) Soil carbon saturation: concept, evidence and evaluation. Biogeochemistry 86:19–31

Strong D, Wever HD, Merckx R, Recous S (2004) Spatial location of carbon decomposition in the soil pore system. Eur J Soil Sci 55:739–750

Subke J-A, Hahn V, Battipaglia G, Linder S, Buchmann N, Cotrufo MF (2004) Feedback interactions between needle litter decomposition and rhizosphere activity. Oecologia 139:551–559

Thomsen IK, Schjønning P, Olesen JE, Christensen BT (2003) C and N turnover in structurally intact soils of different texture. Soil Biol Biochem 35:765–774

Torn MS, Trumbore SE, Chadwick OA, Vitousek PM, Hendricks DM (1997) Mineral control of soil organic carbon storage and turnover. Nature 389:170–173

Trumbore S (2000) Age of soil organic matter and soil respiration: radiocarbon constraints on belowground C dynamics. Ecol Appl 10:399–411

van Delden L, Rowlings DW, Scheer C, De Rosa D, Grace PR (2018) Effect of urbanization on soil methane and nitrous oxide fluxes in subtropical Australia. Glob Change Biol 24:5695–5707

Wattel-Koekkoek E, Van Genuchten P, Buurman P, Van Lagen B (2001) Amount and composition of clay-associated soil organic matter in a range of kaolinitic and smectitic soils. Geoderma 99:27–49

Weier K, Doran J, Power J, Walters D (1993) Denitrification and the dinitrogen/nitrous oxide ratio as affected by soil water, available carbon, and nitrate. Soil Sci Soc Am J 57:66–72